Continental Shelf Research 110 (2015) 48–59

Contents lists available at ScienceDirect

Continental Shelf Research

journal homepage: www.elsevier.com/locate/csr

Research papers

Response of the Bight of Benin (Gulf of Guinea, West Africa) coastline to anthropogenic and natural forcing, Part1: Wave climate variability and impacts on the longshore sediment transport

R. Almar [a,*], E. Kestenare [a], J. Reyns [b], J. Jouanno [a], E.J. Anthony [c], R. Laibi [d], M. Hemer [e], Y. Du Penhoat [a,f], R. Ranasinghe [b,g,h]

[a] LEGOS (CNRS-IRD-CNES-University of Toulouse), Toulouse, France
[b] UNESCO-IHE, Delft, The Netherlands
[c] CEREGE, Aix en Provence, France
[d] Université Abomey Calavi, Département des Sciences de la Terre, Cotonou, Benin
[e] CSIRO Oceans and Atmosphere Flagship, Hobart, Australia
[f] ICMPA-UNESCO Chair International Chair in Mathematical Physics and Applications, Cotonou, Benin
[g] Harbour, Coastal and Offshore Engineering, Deltares, Delft, The Netherlands
[h] Research School of Earth Sciences, The Australian National University, Canberra, Australia

ARTICLE INFO

Article history:
Received 6 December 2014
Received in revised form
10 September 2015
Accepted 28 September 2015
Available online 30 September 2015

Keywords:
Longshore drift
Coastal erosion
Regional wave climate
South Atlantic Ocean
Southern Annular Mode
Inter-Tropical Convergence Zone

ABSTRACT

The short, medium and long-term evolution of the sandy coastline of the Bight of Benin in the Gulf of Guinea, West Africa, has become a major regional focal point due to the rapid socio-economic development that is occurring in the region, including rapid urbanization and a sharp increase in harbor-based trade. Harbors have a significant impact on the present evolution of this coast, notably by affecting longshore sediment transport. However, little is known of the environmental drivers, notably the wave climate, that governs longshore sediment transport and the ensuing pattern of shoreline evolution of this coastal zone. This article aims to address this important knowledge gap by providing a general overview of coastal evolution in the Bight of Benin and the physical processes that control this evolution.

Here, the 1979–2012 ERA-Interim hindcast is used to understand the temporal dynamics of longshore sediment transport. Oblique waves (annual average H_s=1.36 m, T_p=9.6 s, S-SW incidence) drive an eastward drift of approximately 500,000 m^3/yr. The waves driving this large longshore transport can be separated into two components with distinct origins and behavior: wind waves generated locally in the Gulf of Guinea and swell waves generated in the southern hemisphere sub- (30–35°S), and extra-tropics (45–60°S). The analysis undertaken here shows that the contribution to the gross annual longshore transport from swell wave-driven longshore currents is an order of magnitude larger than the local wind wave-driven longshore currents. Swell waves are dominantly generated by westerlies in the 40–60°S zone and to a lesser extent by trade winds at 30–35°S. The longshore sediment drift decay (−5% over 1979–2012) is found to be linked with a decrease in the intensity of westerly winds associated with their southward shift, in addition to a strengthening of the trade winds, which reduces the eastward sediment transport potential. The equatorial fluctuation of the Inter-Tropical Convergence Zone (ITCZ) is found to explain most of the variability in transport induced by wind waves, while the Southern Annular Mode (SAM), an extra-tropical mode, has a predominant influence on transport induced by swell waves. The ITCZ and SAM have, respectively, a negative and positive trend over the period 1979–2012 that explains the decrease in both wind- and swell-wave-induced transport. For future scenarii, General Circulation Models (GCMs) predict a stabilization of the SAM, and, thus, a non-substantial or weak change in longshore sediment transport can be expected on the coast of the Bight of Benin.

1. Introduction

The vulnerability of tropical coastlines is currently increasing under the growing twin pressures of environmental hazards and

* Corresponding author.
E-mail address: rafael.almar@ird.fr (R. Almar).

http://dx.doi.org/10.1016/j.csr.2015.09.020
0278-4343/

human activities. This situation is aggravated in developing countries where rapid economic development is associated with strongly increasing demographic pressure, especially on coasts, and with uncontrolled exploitation of resources (e.g. sand mining and river dams). The available literature regarding the coastal processes that affect tropical coastlines is scarce in general (Short, 2012), and literature on potential impacts of climate change on tropical coastlines, other than those of islands, is practically non-existent. There is, therefore, a pressing need for a better understanding of the present dynamics and future evolution of tropical coasts related to global climate change (ALOC-GG, 2011 report; global warming impact IPCC, 2014 report; Stive, 2004).

This article focuses on the Bight of Benin coast, much of which comprises low-lying barrier-lagoon systems and river deltas (Anthony, 1995) and concentrates about 80% of the regional economic activity in this African sub-region (UEMOA report, 2009). Over 70% of the population of the West African countries bordering the Bight of Benin (Côte d'Ivoire, Ghana, Togo, Benin, and Nigeria, Fig. 1a) lives in the coastal zone. This open sandy bight coast faces a narrow and irregular continental shelf, and is exposed to a wave climate characterized by energetic swell from the South Atlantic and locally-generated short-crested waves (Davies, 1980; Degbe et al., 2010; Yao et al., 2010). The longshore sediment transport (or littoral drift) has been reported to be one of the largest in the world, variably estimated at between 400,000 and 1,000,000 m^3 /yr and directed eastward. These estimates are based on various approaches, including empirical formulae and measurement of sand volumes trapped in the lee of port breakwaters (Tastet et al., 1985; Blivi, 1993; Anthony and Blivi, 1999; WLDelft Hydraulics, 1990). The morpho-sedimentary evolution of the Bight of Benin coast is controlled by this strong longshore sediment transport, resulting in a so called'drift-aligned' coastline (Anthony, 1995; Anthony and Blivi, 1999; Laibi et al., 2014; Anthony, 2015), in the sense of Davies (1980). Although large stretches of the Gulf of Guinea coast, especially the Bight of Benin (Fig. 1), are considered to be in morpho-sedimentary equilibrium (alongshore sand inputs are compensated by alongshore sand outputs at any point) (Anthony, 1995; Anthony et al., 2002; Laibi et al., 2014) with a coastline that is more or less stable over the long-term (10^2–10^3 yr), given the magnitude of the longshore sediment transport rates, any temporary and even minor alongshore disequilibrium in such rates can result in massive local erosion or accretion (Rossi, 1989). Local areas of disequilibrium have been generated over the last few decades especially following the construction of deep-water harbour breakwaters, fundamental to the growing commercial exchanges of the region, and hydropower dams. Even though the impacts of this socio-economic development are manifest in terms of coastal erosion and accretion, the spatial and temporal functioning of the drift system they perturb remains poorly known. This poor state of knowledge has a negative feedback effect on development inasmuch as decision-makers do not appreciate the importance of the medium-tem (order of years) coastal sediment balance and its relationship to current and future development projects. Because the four countries in the Bight of Benin are facing the same vulnerability to erosion, this problem is rapidly becoming a major regional issue (Appeaning Addo, 2009, 2011; Anthony, 2015; Convention d'Abidjan-Mission d'Observation du Littoral Ouest Africain (MOLOA) first report, MOLOA, 2013).

A second gap needing to be addressed, in order to design effective counter-measures for existing and potential future coastal erosion problems, is the severe lack of knowledge (and/or interest) on the climatic drivers (and their potential climate change-driven variations) of wave conditions which, in turn, drive the afore-mentioned longshore sediment transport. Whereas mid- to high latitude climates are strongly dominated by short-event to seasonal processes, tropical to sub-tropical climates in cyclone-free regions are commonly dominated by longer seasonal to inter-annual fluctuations. Due to limited long-term observations, the link between coastal evolution and regional climatic modes has largely remained outside the scope of coastal studies. Only recently have a number of studies started addressing this key link. Pioneer studies on the US west coast (Inman et al., 2001; Allan and Komar, 2002) showed the effect of the El Nino Pacific mode on storm occurrence and impact on inter-annual coastal evolution, with an observed reversal of the longshore drift. On the east coast of Australia, Ranasinghe et al. (2004) demonstrated the influence of the South Oscillation Index on pocket beach rotation, later supported by work undertaken by Harley et al. (2011a), Splinter et al. (2012) and Short et al. (2012). In Europe, the North Atlantic Oscillation (NAO) has been shown to explain most of the inter-annual wave variability in energy and direction (Charles et al., 2012; Masselink et al., 2014) which influences shoreline evolution, although no clear link has been reported by these authors at longer timescales, suggesting a complex response of the coastal system to these climatic variations. However, a link between coastal evolution, North Atlantic waves, and the NAO has been demonstrated for the muddy wave-exposed mangrove coast of French Guiana (Walcker et al., 2015). The South Atlantic Ocean wave regime has attracted much less attention (Hemer et al., 2010) compared to other ocean basins. This is partly due to sparse in-situ observations of winds and waves, a problem now being tackled by the production of increasingly more accurate model hindcasts and by satellite altimetry (Woolf et al., 2002; Young et al., 2011).

This article, which is part one of a series of two, aims to provide general insights on the contemporary and potential future longshore drift regime in the Bight of Benin and associated wave climate forcing using wave hindcasts and future climate projections.

2. Study area

2.1. The Bight of Benin coastline

The study area, comprises the sandy coast between Ghana and Nigeria that forms the Bight of Benin in the Gulf of Guinea, West Africa (Fig. 1). This coast exhibits a mildly embayed sand barrier system between the western confines of the Niger River delta in the east and the Volta River delta in the west (Anthony and Blivi, 1999; Anthony et al., 2002). It is an open environment exposed to long swell waves that travel far from mid- to high latitudes (45–60°) in the South Atlantic as well as to locally generated short-waves in the tropical band (6°N to 15°S). The mid- to high-latitude wind regime is characterized by strong westerlies whereas the subtropical area (30–35°S) is dominated by south easterly trade winds blowing off the coast of Namibia. The southwesterly swells impinge slightly obliquely (at angles of 10–15°) on the nearly rectilinear west-east oriented Bight of Benin coast, generating the afore-mentioned unidirectional and large longshore drift toward the east. The tidal regime is microtidal (from 0.3 m to 1.8 m for neap and spring tidal ranges, respectively).

The beaches along this coast (Almar et al., 2014; Laibi et al., 2014) are mostly in the 'reflective-to-intermediate' state classes (Gourlay parameter, $\Omega = 1$, following Wright and Short, 1984; Relative Tide Range RTR$\sim$1, Masselink and Short, 1993), and often exhibit an alongshore-uniform low-tide terrace and a steep reflective upper beachface (Fig. 1d). The grain size is medium to coarse with $D_{50} = 0.6$ mm (Anthony and Blivi, 1999).

2.2. South Atlantic climate dynamics

In this section the different modes of climate variability in the South Atlantic that affect winds and waves and subsequently the

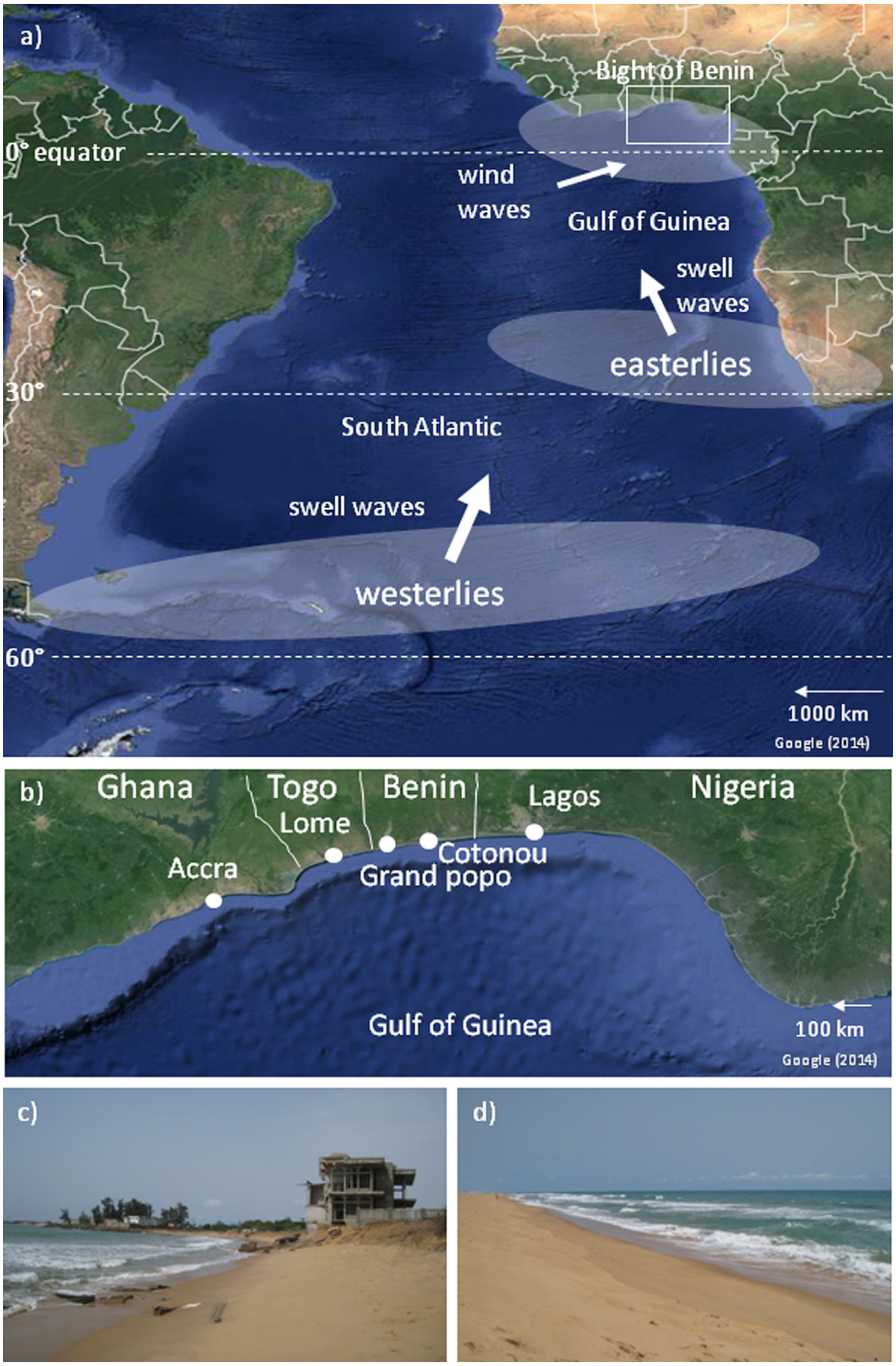

Fig. 1. The Bight of Benin coast, showing the four countries sharing this coast, and the sites of Grand Popo and Cotonou (Benin) (a); South Atlantic Ocean and (b) Gulf of Guinea regional map, corresponding to white square in (a). (c, d) ground photographs of part of the eroding sector of Cotonou and the stable sector of Grand Popo.

longshore sediment transport rates in the Bight of Benin are reviewed.

2.2.1. Southern Atlantic

Hemer et al. (2010) found that wave height in the Atlantic sector of the Southern Ocean is negatively correlated with the Southern Annular Mode (SAM) during the southern hemisphere winter, with positive anomalies of the SAM corresponding to a decrease in wave height and a small anticlockwise rotation of dominant wave direction (Fig. 2). This contrasts with the Pacific sector of the Southern Ocean where both wave height and direction are significantly and positively correlated with the SAM, with increased wave height when the SAM is positive. The SAM appears to have a strong influence at latitudes where the largest waves in the Southern Ocean are found (e.g., Bosserelle et al., 2012). A positive SAM is associated with an increased atmospheric pressure gradient between mid- and high latitudes. These atmospheric conditions tend to prevent storms from tracking northward to the mid- latitudes and thus force wave events to remain at latitudes south of 50°S.

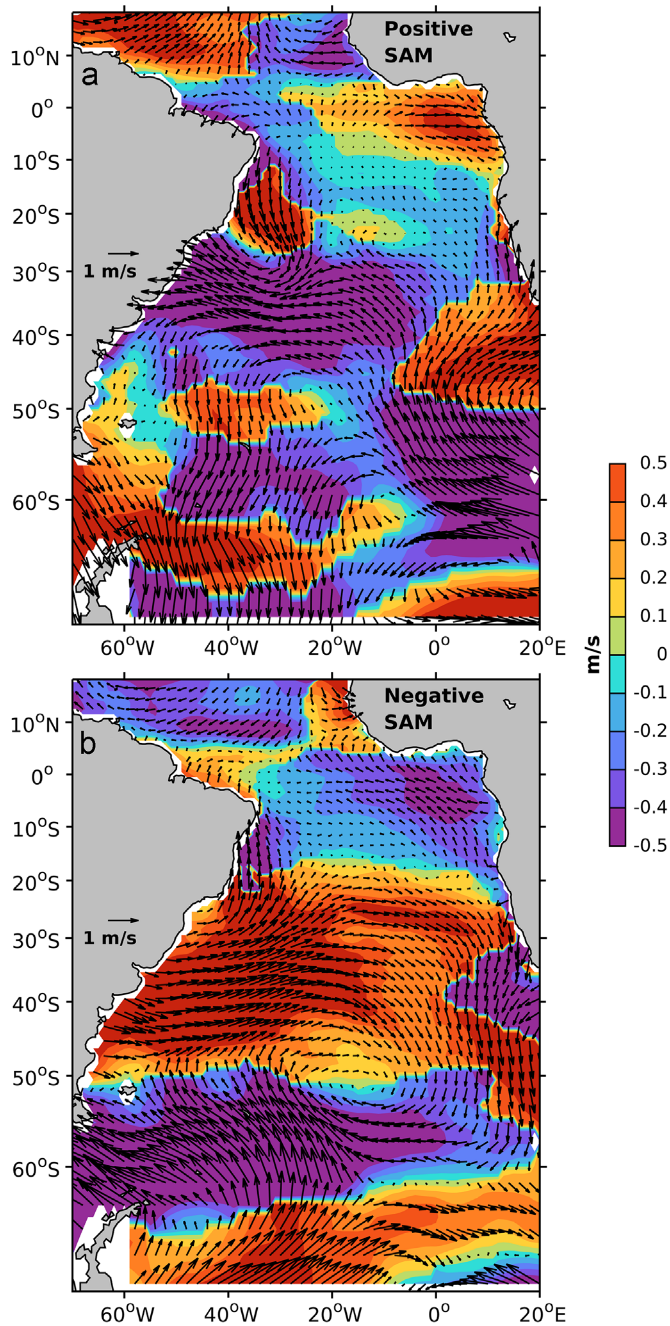

Fig. 2. Composite map of South Atlantic winds (arrows, m/s) and zonal wind components (colors, m/s) anomalies for: (a) a positive SAM and (b) negative SAM, computed from largest SAM events (greater than $\pm$ 1.6 times standard deviation). (For interpretation of the references to color in this figure legend, the reader is referred to the web version of this article.)

The positive trend in the SAM observed over the past few decades is associated with an intensification of the Southern Ocean storm belt (Marshall, 2003), leading to an increase in wave height in the far Southern Ocean (Hemer et al., 2010). However, trends in the wave climate of the Southern Ocean display strong regional variability. Particularly in the South Atlantic, the long-term evolution of wave height shows opposite tendencies, depending on the wave-product that is considered (see Fig. 8 in Hemer et al., 2010), and therefore, the impact of the positive trend of the SAM is less clear in this sector of the Southern Ocean. The Southern Ocean synoptic atmospheric eddies, which are at the origin of the largest swells in the southern hemisphere, tend to occur preferentially in particular paths that have been referred to as "storm tracks". Hoskins and Hodges (2005) have shown that the southern hemisphere summer storm track is a single, deep concentrated high-latitude entity, whereas the winter track also has a subtropical component, with intense synoptic wave activity along the subtropical jet. Two subtropical genesis regions have been identified near 30°S and 45°S off South America. Similarly, Mendes et al. (2011) identified two clusters of cyclone tracks in the Southern Atlantic: northeast Argentina and north of the Antarctic Peninsula (around the Weddell Sea). These authors observed an influence of the SAM in the location of extra-tropical cyclones around 40°S, while the impact on the intensity is detected around 55°S. Although it has been well known for decades that energetic swells travel from the South Atlantic to the Gulf of Guinea (Sitarz, 1960), it is still unclear which of these clusters exerts the dominant control on wave energy flux to the coasts of the Gulf. Using NCEP–NCAR reanalysis, Fyfe (2003) has shown a poleward shift of the storm track over the last decades, leading to less cyclones in the Sub-Antarctic Ocean (north of 40°S) and a slight increase in the number of cyclones in the Antarctic Ocean. This is in agreement with the study of Rao et al. (2003), who showed that the negative correlation found in the subtropical storm track region between the SAM and the growth rate of synoptic eddies is due to a reduction in the wind shear and an increase in the static stability. Sterl and Caires (2005) associated the general increase in wave height over the Southern Ocean in the past few decades with an increased number of storms in this ocean.

The analysis of Hemer et al. (2010) also revealed a weak correlation between Atlantic wave height and the Southern Oscillation Index (SOI), in contrast to the Pacific where the El Nino Southern Oscillation (ENSO) is shown to have a great impact on the wave-energy flux. Examining inter-annual variability of wave direction at a specific location close to northern Argentina, Solari and Losada (2012) found an influence of the SAM and Tropical Southern Atlantic (TSA) on wave directions in Uruguay while the influence of ENSO was found to be very weak.

2.2.2. *Equatorial and tropical Atlantic*

The dominant mode of inter-annual variability in the equatorial Atlantic shares characteristics with ENSO, with an inter-annual alternation of cooling and warming of surface ocean temperature in the eastern part of the basin (0–30°W) related to changes in the trade winds. A warm anomaly is associated with weaker trade winds across the equatorial Atlantic basin, whereas a cool anomaly is associated with enhanced easterly winds. The winds along the northern Gulf of Guinea are predominantly from the southwest. Fluctuations of the St. Helen anticyclone can lead to 15-day wind bursts that can reach the northern Gulf of Guinea (e.g. de Coetlogon et al., 2010). Moreover, the low-elevation winds of the equatorial Atlantic are influenced by high-frequency equatorially trapped waves (e.g. Wheeler and Kiladis, 1999). Using bias-corrected observations over the last six decades, it has been shown that a long-term warming of the eastern Atlantic leads to less vigorous trade winds (Tokinaga and Xie, 2011). Richter et al. (2014) have shown a very high correlation between the latitudinal ITCZ position and the strength of the equatorial easterlies as illustrated in Fig. 3. They show that, from the equator to 15°N, the equatorial easterlies intensify quite linearly with ITCZ displacement over the same latitudinal range. Okumura and Xie (2004) have shown a link between equatorial upwelling, southerly strengthening and southerly displacement of the ITCZ, but the link between the variability of these systems is not completely understood (Richter et al., 2014). Atlantic Niño are associated with south equatorial excursion of the marine ITCZ (Xie and Carton, 2004; Richter et al., 2014), accompanied by northwesterly surface wind anomalies. In Section 4.2, we will discuss the potential links between these

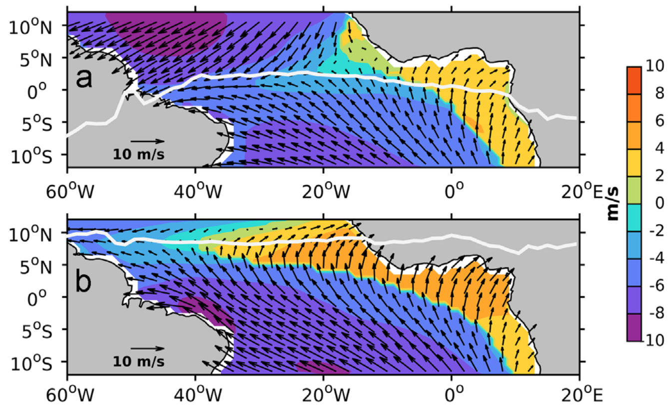

Fig. 3. Atlantic equatorial wind field (m/s) associated with: (a) southernmost position of the ITCZ and (b) northernmost position of the ITCZ. Thick white line shows mean position of the maximum of precipitation below the ITCZ.

various modes of variability and longshore sediment transport rates in the study area.

3. Data and methodology

3.1. Waves

In order to estimate the wave-induced longshore transport on the Bight of Benin coast, we use bulk wave parameters (significant height H_s, peak period T_p and direction of both swell and wind waves) derived from hindcast data in the Atlantic Ocean between 1979 and 2012, generated by the ECMWF Wave Atmospheric Model (WAM) model (The Wamdi Group, 1988). These wave data are part of the ERA-Interim dataset, which involves a reanalysis of global meteorological variables (Dee et al., 2011; Sterl and Caires, 2005). Wave data were extracted from the ECMWF data server on a $0.5° \times 0.5°$ grid, with a 6-h temporal resolution. The ERA-40 and the following ERA-Interim reanalysis are the first in which an ocean wind-wave model is coupled to the atmosphere, and the quality of the wave data has been extensively validated against buoy and altimeter data. Sterl and Caires (2005) demonstrated a very good correlation between the ERA-40 data and these sources, except for very high waves ($H_s > 5$ m) and very low waves ($H_s < 1$ m), which tend, respectively, to be under- and over-estimated (Caires et al., 2006). Fortuitously, these extreme wave conditions are not typically observed in the relatively constant wave regime of the Gulf of Guinea. However, the South Atlantic Ocean remains one of the most remote locations on earth with scarce observations, and this affects the hindcast quality. ERA-40 and -Interim results for this region therefore need to be treated with caution.

Future projected wave climate scenarios were used to estimate future projections of longshore drift. The future wave climate scenarios were derived from dynamical wave climate projections, whereby a global 1° resolution implementation of the WaveWatch III spectral wave model (v3.14; Tolman, 2009), using BAJ (Bidlot et al., 2007) source terms, was forced with 3-h surface winds and monthly sea-ice concentration fields taken from an ensemble of CMIP-5 General Circulation Models (GCMs). Hemer and Trenham (2015) report on the skill of the eight historical CMIP-5 GCM forced wave simulations which span 1979–2005. In this study we use results from accompanying future scenario simulations which were carried out using the same 8 GCMs (ACCESS1.0, BCC-CSM1.1, CNRM-CM5, GFDL-CM3, HadGEM2-ESM, INMCM4, MIROC5, MRI-CGCM3), for two future time-slices (mid 21st Century 2026–2045; and end 21st Century 2081–2099), considering two different emission scenarios (RCP4.5 and RCP8.5) in each time-slice. These simulations provide are a contribution to the second phase of the Coordinated Ocean Wave Climate Project, following Hemer et al., 2013). Bulk parameters (H_s, T_p, and mean wave direction) are archived at 6-h temporal resolution globally. In the present paper, we extract the 6-h time-series for the grid cell nearest the Bight of Benin, and use monthly averages of the bulk parameters over the region.

3.2. Longshore sediment transport

There are several bulk longshore transport formulations that are widely applied by coastal engineers. These are, among others, the CERC (1984), Kamphuis (1991), and the more recently developed Kaczmarek et al. (2005) formulae. There is still an ongoing research effort on the improvement of bulk longshore sediment transport equations (see for example, Mil-Homens et al., 2013) and there is no general consensus on the choice of a formulation. Here, we chose the recent Kaczmarek et al. (2005) formula due to its suitability for remote sites such as the Bight of Benin where only limited observations exist. Furthermore, this formula has previously been applied to similar environments (Bertin et al., 2008). In this formula, the sediment volume transported alongshore is computed as:

$$Q = 0.023 - h_b^2 V \quad \text{if} \left(h_b^2 V\right) < 0.15, \tag{1}$$

$$Q = 0.00225 + 0.008(h_b^2 V) \quad \text{if} \, (h_b^2 V) > 0.15 \tag{2}$$

where h_b is the breaking wave height and V an estimated longshore current within the surf zone derived from the commonly used Longuet-Higgins (1970) formula:

$$V = 0.25 k_v \sqrt{\gamma g h_b} \sin 2\alpha_b \tag{3}$$

where α_b is the local breaking wave angle, $\gamma = h_b/d_b = 0.78$ the constant breaker index following Battjes and Janssen (1978), g the gravitational acceleration (m/s²), d_b the local water depth, and k_v an empirical constant. Here, we used $k_v = 2.9$ based on the values suggested by Bertin et al. (2008) for wave-dominated environments with similar grain size characteristics. Wind–wave and swell-wave-induced longshore sediment transport were calculated separately and the results obtained were compared with lonsghore sediment transport rates computed by the more commonly used CERC (1984) and Kamphuis (1991) estimations to gain confidence in the former calculations.

Longshore sediment transport formulae require as input the breaking wave parameters, but global wave hindcasts only provide deepwater characteristics. Our study focuses on regional large-scale and seasonal to inter-annual variations over a long period of 34 yr. Although using a nested numerical model (e.g. SWAN or WW3) to propagate waves from deepwater to the breakpoint would have been an ideal option for a short-term study, because of the difficulties presented by the spatio-temporal scales of this study, we have used here the empirical breaking wave predictor proposed by Larson et al. (2010). This formula directly provides breaking wave height h_b and angle α_b, given deepwater wave height h_o, period T and direction α_0:

$$h_b = \lambda C^2 / g \tag{4}$$

$$\alpha_b = a \sin(\sin(\alpha_0)\sqrt{\lambda}) \tag{5}$$

with a correction factor λ computed as:

$$\lambda = \Delta\lambda_a \tag{6}$$

considering

$$\Delta = 1 + 0.1649\xi + 0.5948\xi^2 - 1.6787\xi^3 + 2.8573\xi^4 \tag{7}$$

$$\xi = \lambda_a \sin\theta_0^2,\ \lambda_a = [\cos(\alpha_0)/\theta]^{2/5},\ \theta = \left(\frac{C}{\sqrt{gH}}\right)^4\left(\frac{C}{C_g}\right)\gamma^2 \tag{8}$$

where deep water phase celerity is given by $C=1.56\,T$, wavelength $L=1.56\,T^2$, and group celerity $C_g=C/2$.

3.3. Other data

Wind at 10 m, mean sea level pressure, and precipitation fields, were extracted from ERA-Interim (0.5° × 0.5°grid, every 6 h) over the same 1979–2012 duration used for waves. Wind and pressure fields were used to describe wave generation conditions. Precipitation was used to estimate the location of the monthly Inter-Tropical Convergence Zone (ITCZ) index defined as the longitude-averaged (10°W to 5°E) latitude location of the maximum precipitation, following previous studies (de Coëtlogon et al., 2010). Monthly values of the Southern Oscillation Index (SOI) and the Atlantic Nino or Atlantic Meridional Mode (AMM) were provided by the United States National Oceanic and Atmospheric Administration (NOAA[1,2]), and the Southern Annular Mode (SAM) by the British Antarctic Survey (BAS[3]) (Marshall, 2003). To locate the generation regions responsible for sediment transport in the Bight of Benin, we computed correlations between, on the one hand, daily strong winds of magnitudes greater than 1.6 multiplied by the standard deviation of extreme events (values not changing substantially between 1.4 and 1.8, 1.6 allow retaining ~10% of dates) in the South Atlantic (10° × 10° cells), and, on the other, longshore sediment transport at Cotonou, in the center of the Bight of Benin coast (Fig. 1b).

In order to describe the evolution of the shoreline at the regional scale in the Bight of Benin, LANDSAT 5, 7 and 8 imagery (USGS, 2014) was used. These images have a grid resolution of 30 m in the spectral bands, and are referenced in the UTM WGS84 system (USGS, 2014). For the years 1985, 1990, 2000, 2005, 2010 and 2014, satellite images with minimal cloud coverage over the area of interest were extracted. As a discrepancy in the georeferencing over time was noted during the analysis, all images were referenced to the 2014 image using clearly visible reference points that were identifiable in the entire time series. As the ultimate focus herein is on relative shoreline position changes, this approach will have no effect on the final result. Shorelines were digitized using a band combination maximizing shoreline contrast. For the present paper, the focus was on two representative sites of the Bight of Benin coastline (Fig. 1): Grand Popo (Fig. 1d), considered as unperturbed as it is sufficiently far from any harbour influence, and Cotonou, characteristic of an anthropogenically impacted sector of coast with shoreline erosion (Fig. 1c) downdrift of the deepwater harbour. At each site, a ~20 km stretch of coastline was extracted and shoreline evolution was computed.

4. Results and discussion

4.1. Wave climate and longshore drift

4.1.1. Wave climate

Averaging all waves over the period 1979–2012 yields an annual significant wave height of H_s= 1.36 m, a peak period of T_p =9.4 s, and a dominant S-SW direction (189° clockwise from north). Seasonal modulation of swell waves is weak, with H_s peaking at 1.6 m during austral winter (Fig. 4) that coincides with strong westerlies at mid latitudes. The annual average wind wave H_s is smaller (0.4 m) and the direction is more oriented from the west (215° from north). Wind waves also show larger day-to-day and monthly variations. Contrary to the swell waves, wind waves are driven by local tropical winds and show two annual peaks, one in March and a larger one in July. The peaks correspond to the extreme locations of the ITCZ, the passage of the ITCZ over the Bight of Benin coastline being associated with weaker winds. Fig. 4 also shows that the wave climate is rather uniform within the Gulf of Guinea and particularly along the open coastline of the Bight of Benin. It is important to note that several wave trains are often concomitant in the Gulf of Guinea even though the energy peak is dominated by long southwest swells. This is due to the coast being far enough from the swell generation zone to be affected by both local and distant waves, which facilitates the coexistence of multiple wave-generation zones. The effect of secondary waves might therefore be underestimated if only the main swell component is considered.

4.1.2. Longshore sediment transport and coastline evolution

Both swell and wind waves are dominantly incident from S-SW. This results in an oblique (5–15°) wave incidence at the coastline, generating a large transport toward the east. Fig. 5 shows the annual longshore sediment transport (LST) in the Bight of Benin for the total of swell- and wind-wave contributions computed with the Kaczmarek et al., (2005) formula. In the center of the Bight of Benin at Cotonou (Fig. 1), the annual net transport induced by swell waves is 453,000 m^3/yr and the wind-wave induced transport is 63,000 m^3/yr, an order of magnitude smaller. The CERC (1984) estimates for the same quantities are more or less the same (455,000 and 48,000 m^3/yr respectively), while estimates given by the Kamphuis (1991) formula are larger, but of the same order of magnitude (630,000 and 21,000 m^3/yr respectively). Seasonal variations in longshore sediment transport are weak due to limited seasonal changes in wave energy and direction. A convergence zone is observed at (6.25°N, 4.5°E), east of Lagos, Nigeria, both for swell- and wind-wave-induced longshore transport. This is due to the alongshore variation in the local incidence angle of waves relative to the shoreline orientation rather than wave direction, which is almost uniform along the coast.

Fig. 6 shows the interannual variation of the swell- and wind-wave-induced longshore sediment transport at Cotonou. It can be seen that for both components the year-to-year variability is large and a decreasing trend of 680 and 850 m^3/yr is observed for swell- and wind-wave-induced longshore transport (significant at 90% and 99% levels using the Mann Kendall test), respectively (total combined decreasing trend of 1530 m^3/yr, compared with 1693 and 1430 m^3/yr for CERC (1984) and Kamphuis (1991), respectively). This amounts to a 5% decrease in total net longshore transport over the 1979–2012 study period.

The coastline evolution over the same period at Cotonou and Grand Popo, Benin, which are 80-km apart, is shown in Fig. 7. The undisturbed Grand Popo coastline (Fig. 7a and c) is rather stable during this period whereas the coastline at Cotonou, which is interrupted by a large harbour, shows updrift accretion (+3.5 m/yr, total +102 m) and downdrift erosion (−7.3 m/yr, total −212 m;

[1] www.cpc.ncep.noaa.gov/data/indices/soi.
[2] www.esrl.noaa.gov/psd/data/timeseries/monthly/AMM.
[3] www.nerc-bas.ac.uk/icd/gjma/sam.html.

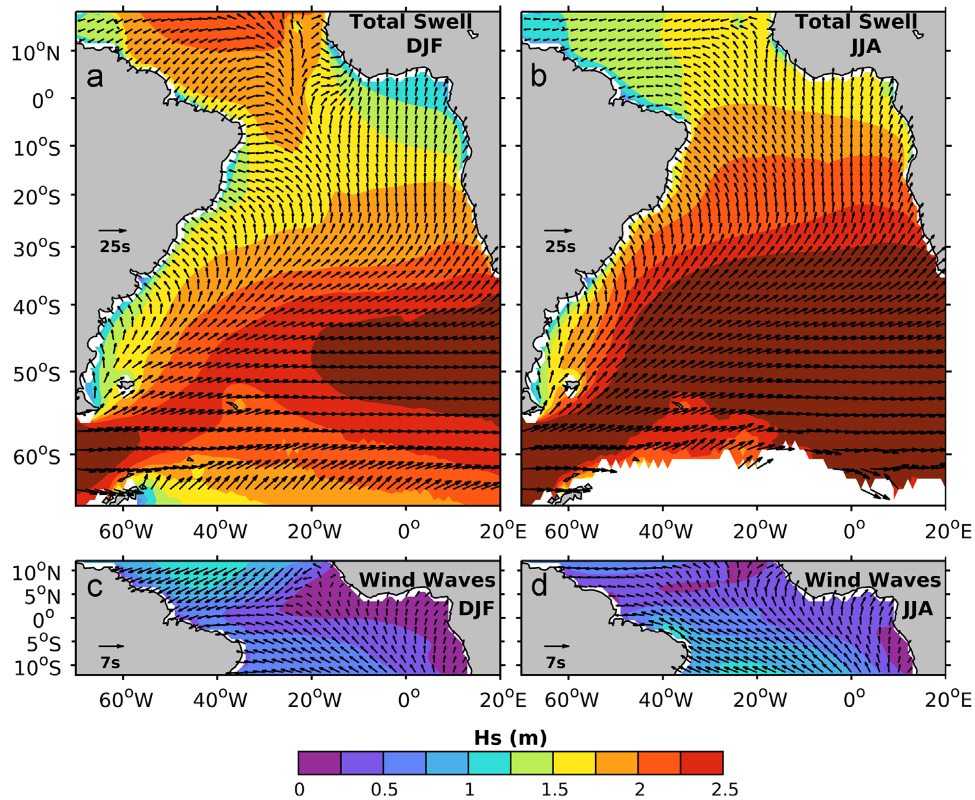

Fig. 4. Average wave conditions during the southern hemisphere summer (DJF) and winter (JJA) in the South Atlantic Ocean (a and b) and in the Equatorial Atlantic Ocean (c and d). Significant wave height is in color, period and direction are represented by arrows length and orientation, respectively. (For interpretation of the references to color in this figure legend, the reader is referred to the web version of this article.)

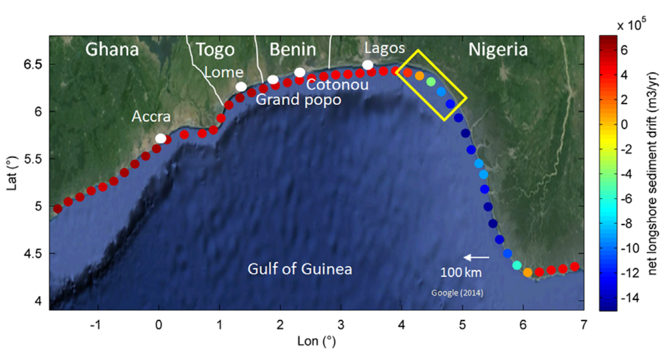

Fig. 5. Net annual longshore sediment transport in the Bight of Benin induced by the total contribution of swell waves. Positive values towards the east. Yellow rectangle shows transport convergence region. (For interpretation of the references to color in this figure legend, the reader is referred to the web version of this article.)

Fig. 7b and c). Even if it may be hazardous to link directly the observed evolution of the coastline to the alongshore drift gradient, it is reasonable that for a constant sediment supply, from the Volta River and involving exchanges with shelf, the observed reduction in drift contributes to a relative stabilization of the coastline due to the weaker longshore sediment transport gradients. The large 9 m/yr coastline change rate (averaged over absolute values of updrift accretion and downdrift erosion) observed at Cotonou (Fig. 7c) during the period 1985–1990 decreases by more than 50% to 4 m/yr over the 2010–2014 period. Part of this trend may be attributed to the decrease in longshore sediment transport (Fig. 6) but also to the long-term morphological stabilization around the harbour. This aspect is addressed in more detail in an upcoming part 2 paper which focuses on the multi-scale geomorphologic evolution of the Bight of Benin.

In the following section, we describe the main drivers of the observed spatio-temporal variations in longshore sediment transport, and their possible links to modes of climatic variability.

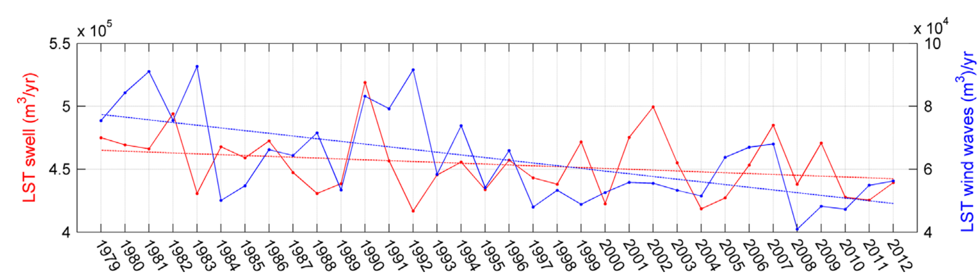

Fig. 6. Inter-annual variation of the net annual longshore sediment transport at Cotonou induced by swell (red) and wind waves (blue). Dashed line shows trend over the period. Note the two different vertical axes for the two types of waves. (For interpretation of the references to color in this figure legend, the reader is referred to the web version of this article.)

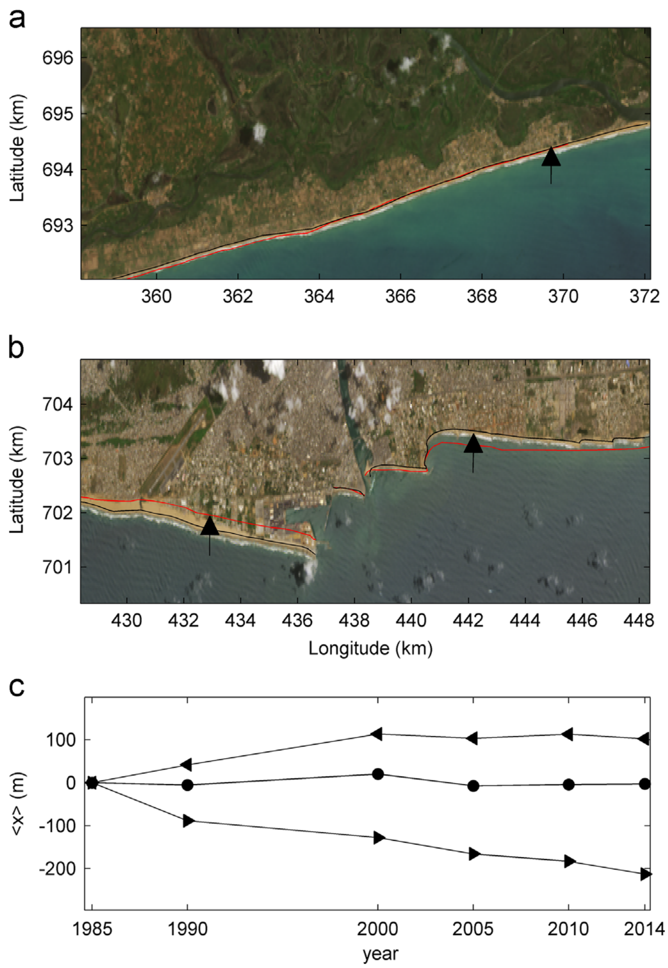

Fig. 7. (a) The shorelines at Grand Popo and (b) Cotonou in 1985 (red) and 2014 (black) superimposed on 2014 LANDSAT 2014; (c) Shoreline evolution from available LANDSAT images over the period 1985–2014 at Grand Popo (circles) and Cotonou, updrift (left-oriented triangles) and downdrift (right-oriented triangles)of Cotonou harbour. (For interpretation of the references to color in this figure legend, the reader is referred to the web version of this article.)

4.2. Potential regional climate influence on alongshore sediment transport

Wind waves are locally generated in the Gulf of Guinea. Swell waves travel larger distances from the zone of generation before reaching the coast. Fig. 8a shows that the largest positive correlations between resulting daily LST and wind fields (see Section 3 for methodology) are found at 40–60°S in the western part of the basin (correlation coefficient >0.5, significant at 95%) with an 8-day lag, whereas a weak negative correlation (-0.2, significant at 95%) with a 6-day lag is found at 30°S in the eastern part of the basin (off the coast of South Africa and Namibia). To further investigate the regional meso-scale atmospheric patterns associated with these wave components, composite lagged wind and pressure maps prevailing just before the occurrence of the maximum of positive and negative sediment transport were constructed (Fig. 9). The results in Fig. 9a and b indicate that both events are due to synoptic-scale mid-latitude dynamics. Swells incident from the West are mainly generated by synoptic anticyclonic storms traveling eastward at 40–50°S (Fig. 9a) whereas easterly swells are generated by cyclonic wind anomalies on the eastern side of the South Atlantic at latitudes of 30–40°S. It is noteworthy that westerly events mostly occur in the southern hemisphere winter whereas fewer easterly events occur in spring-summer. The forcing by westerly swell is dominant, while easterly winds associated with trade-wind perturbations in the eastern basin generate less frequent, but substantial secondary swells. For the wind waves, a composite map of winds and sea level pressure at zero-lag with a maximum of wind-wave transport at Cotonou was computed (Fig. 9c). It shows that this maximum occurs due to a westward wind anomaly centered on the equator and associated with a low-pressure system in the Sahel. This pattern resembles the 10–25 day period ITCZ mode described in Janicot et al. (2011) and linked with the African monsoon system. The anticyclonic/cyclonic composite anomalies identifiable south of 20°S in Fig. 9c could be indicative of equator-extra-tropical remote connection between the intra-seasonal wind in the Gulf of Guinea and the storm-track synoptic variability. Investigating this possible mechanism, while being of potential interest, is however, beyond the scope of this study.

The causes for the decrease in the alongshore sediment transport over the period 1979–2012 observed in Fig. 6 are investigated here. Interestingly, as seen in Fig. 8b, the South Atlantic wind field shows substantial changes with spatially variable behavior over the basin; it is observed to decrease slightly (significant at 99%) in the Gulf of Guinea (-1 cm/s) and more substantially at latitudes between 40 and 50°S (3 cm/s, significant at 99%), but increases elsewhere (c.f. Hemer et al., 2010). Trade winds are observed to be stable or even increase substantially, associated with a strengthening of the Saint Helen anticyclone. Comparing the wind trend map in Fig. 8b with the correlation between wind and sediment transport in the Bight of Benin in Fig. 8a indicates that the reduction of swell-wave generated transport may be attributed to two distinct and concurrent processes: at first order the decrease in south westerly swells generated by mid-latitudes storms, and at second order the increasing contribution of secondary south easterly swells (which will drive westward longshore transport, thus reducing the net eastward longshore transport) generated by positive anomalies in the trade-wind.

As discussed in Section 2, part of the wind variability in the Gulf of Guinea is closely tied to the displacements of the ITCZ. We found a significant correlation (0.4 at zero lag, 95% confidence level) between wind-wave transport and the monthly ITCZ index, consistently with previous findings by Gratiot et al. (2007), while the correlation is weak and insignificant with the SOI and with the Atlantic El Niño. Interestingly, the ITCZ and wind-wave transport have the same tendency. The position of the ITCZ thus plays a primary role in wind-wave transport in terms of variability and trend. Regarding swell-wave transport, a significant negative correlation (-0.3 at 0 lag, 95% confidence level) is found with the monthly SAM index whereas no significant correlation is found with other climatic indices. As discussed above, the reduction of swell-wave generated transport is linked to the reduction of storm activity at mid latitudes, which is further confirmed by the decreasing SAM index value over the 1979–2012 period. These results show that regional climatic modes do play a key role in determining longshore sediment transport rates along the coast and underline the need for better understanding their dynamics and variability.

4.3. Future evolution of sediment transport in the Bight of Benin

For the Southern Hemisphere, CMIP5 models project poleward migration, upward expansion, and intensification of the storm track (Chang et al. 2012), with a significant increase in the frequency of extreme cyclones during the southern hemisphere winter. Projections also indicate that the number of Sub-Antarctic Ocean cyclones will drop by over 30% between now and the end of the century (Fyfe, 2003). Because of the strong influence of the South Ocean on the global wave climate, these changes are expected to impact even remote regions. Wang and Swail (2006) and

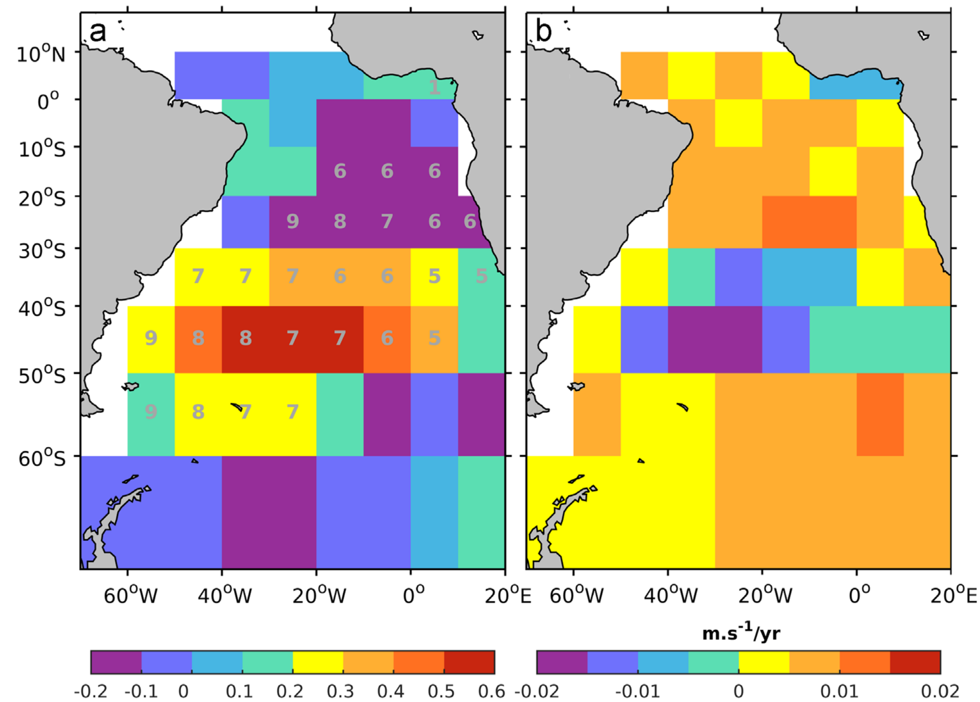

Fig. 8. (a) Maximum lagged correlation between daily wind- and swell-induced transport at Cotonou, over the period 1979–2012. Numbers show the time lag (days) of the maximum of correlation, which indicates the time needed by waves to reach the Gulf of Guinea coast; and (b) Annual average tendency of wind speed($m\ s^{-1}$/yr) over the period 1979–2012.

Hemer et al. (2012) investigated future changes of means and extremes of ocean wave heights using projections of possible future climates. In the Gulf of Guinea, increasing trends of both wave period and wave height can be inferred from the multi-model approach of Hemer et al. (2012). However, Hemer et al. (2013) noted large uncertainties for much of the tropical ocean in their assessment across several wave climate projection studies, with average trends lower than the dispersion between models, such that the confidence in projected wave trends in the Gulf of Guinea remains low.

For the equatorial Atlantic, projections for the 21st century suggest a trend similar to that over the last 3 decades, with warming of the tropical Atlantic and weakening of the trade winds. Projected changes for this area should be treated with caution since most CMIP models simulate a warm bias along the equatorial Atlantic, and the Angola–Namibia upwellings, which impact the low-level atmospheric circulation, are not accurately reproduced (Richter et al., 2014).

Projected South Atlantic wave climate for the 2026–2044 and 2081–2199 periods for low (RCP4.5) and high (RCP8.5) future greenhouse gas emissions scenarii were used to estimate future evolution in the alongshore sediment transport off Cotonou (Fig. 10), including swell and wind wave contributions. Projected seasonal cycles show that summer LST is expected to increase substantially, while the net annual sediment transport will steadily increase compared to the 1979–2012 period, with values of 509, 529 (530) and 537 (567) $10^3\ m^3$/yr respectively for present, RCP4.5 (RCP8.5) mid-century and end-of-the-century periods. A possible explanation may be that the historical SAM-associated trend is unlikely to continue into the future, as the SAM is strongly influenced by tropospheric ozone. As the southern hemisphere ozone levels recover, the SAM will return to a less positive state. Arblaster et al. (2011) show that projected changes in the SAM are a play-off between ozone recovery and greenhouse emissions. In the scenarii with low future greenhouse gas emissions, ozone recovery dominates and the SAM returns to a neutral state. In high greenhouse gas emission scenarios, the SAM tends to be positive, but weaker than it is at present. However, these projections should be taken with caution as a large bias exists in tropical ocean dynamics in the GCMs (Toniazzo and Woolnough, 2014). In Fig. 10 the large discrepancy between the models and the fact that the model ensemble does not capture the present decreasing trend calculated from ERAinterim, nor its interannual variability, underline this uncertainty.

5. Conclusions

This study provides new insights on the contemporary and potential future longshore drift regime in the Bight of Benin, Gulf of Guinea, West Africa, and associated wave climate forcing, using wave hindcasts and future climate projections. The results show that annual averaged wave characteristics in the study area are $H_s = 1.36$ m, $T_p = 9.6$ s with waves dominantly incident from the S-SW, driving a net longshore sediment transport estimated to be 500,000 m^3/yr toward the east. A convergence of this transport was found in the eastern part of the Bight of Benin, east of Lagos, resulting from the spatial variation of coastline orientation. This convergence also marks the transition zone between the longshore sediment transport regimes of the Bight of Benin and the western confines of the Niger river delta, the largest delta in Africa.

The longshore sediment transport was observed to have a substantial decreasing trend over the study period (−5%). The analysis also showed that the longshore sediment transport generated by swell waves is an order of magnitude larger than that generated by wind waves. To understand these patterns, the links between transport and wave forcing, their origins, variability and trends were investigated. An analysis conducted to identify the wave generation zone showed that swell waves are dominantly driven by westerlies in the 40–60°S zone (0.4 correlation coefficient at a 8-day lag) and to a lesser extent by trade winds at 30–35°S (−0.2 correlation coefficient at a 6-day lag), both in close

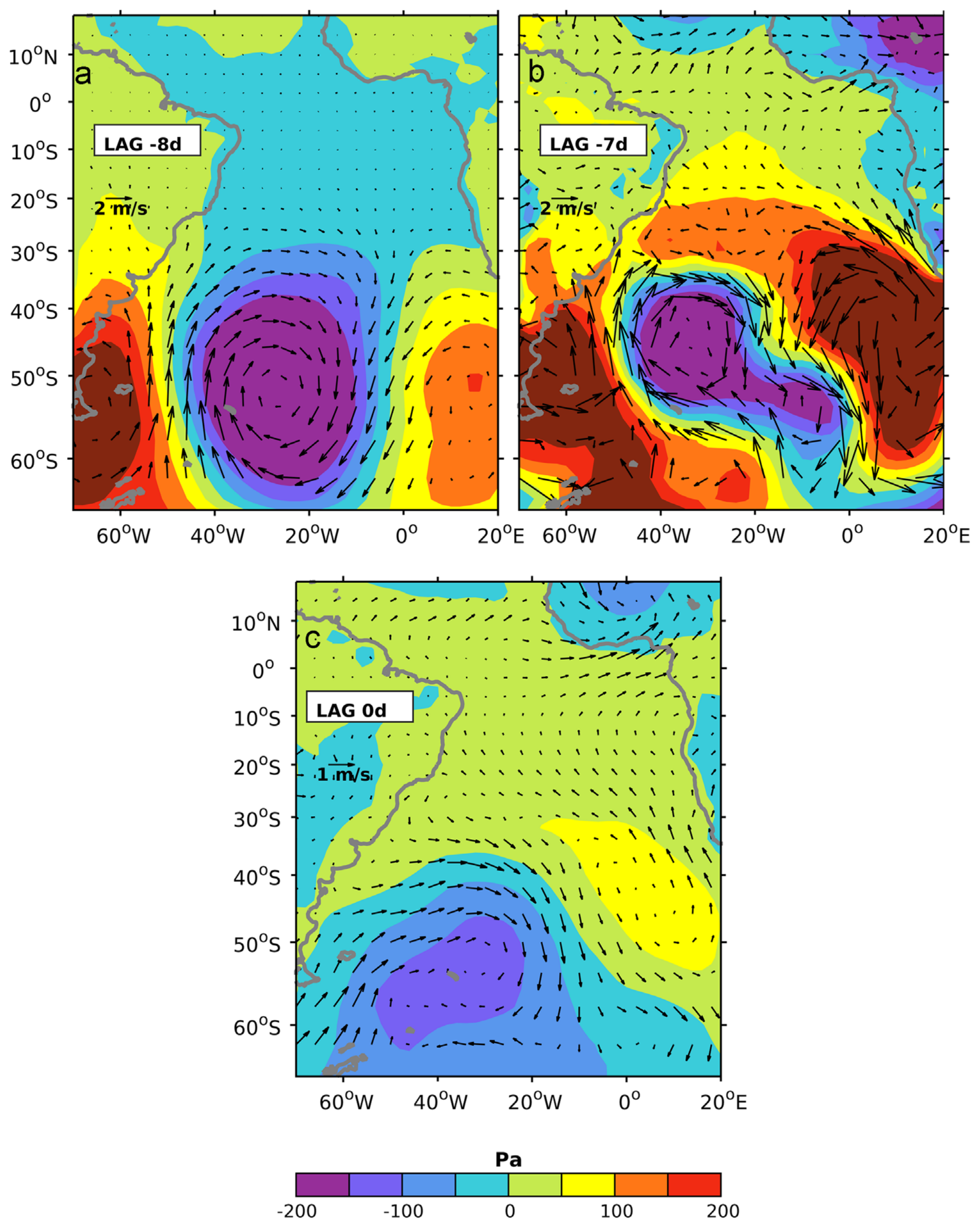

Fig. 9. Composite map of South Atlantic wind (arrows, m/s) and sea level pressure (colors, Pa) anomalies for: (a) 8-day lag before maximum of eastward swell-wave transport; (b) 6-day lag before maximum of westward swell-wave transport; and (c) 0-day lag of maximum eastward wind-wave transport. (For interpretation of the references to color in this figure legend, the reader is referred to the web version of this article.)

interaction with the dynamics of the Saint Helen anticyclone.

The temporal decay in longshore transport was found to be linked with a decrease in the intensity of westerly winds associated with their southward shift, in addition to a strengthening of the trade winds, which reduces eastward sediment transport potential. The equatorial fluctuation of the ITCZ was found to explain most of the variability in transport induced by wind waves, while the SAM extra-tropical mode has a predominant influence on transport induced by swell waves. The ITCZ and SAM have, respectively, a negative and positive trend over the period 1979–2012 that explains the decrease in both wind- and swell-wave-induced transport. For future climate scenarios, GCMs predict a stabilization of the SAM, and, thus, a non-substantial or weak change in alongshore sediment transport can be expected on the coasts of the Bight of Benin.

It should be noted that this study only considers potential future changes in waves. However, future human interventions on the shoreline and future variations in phenomena such as river flow, fluvial sediment supply, mean sea level etc., may also contribute in a complex and non-trivial way to long-term coastline evolution. While this study provides a sound basis for understanding the wave-driven longshore sediment transport regime along the coastline of the Bight of Benin, the robust quantification and prediction of long-term coastline evolution due to all relevant forcing phenomena, as required for effective adaptation and risk reduction, necessitates a thorough consideration of all key physical processes and the different spatio-temporal scales at which the forcing and response mechanisms operate.

Acknowledgments

This study was funded by the French INSU/CNRS LEFE and EC2CO programmes, the IRD (Action Incitative programme), ANR

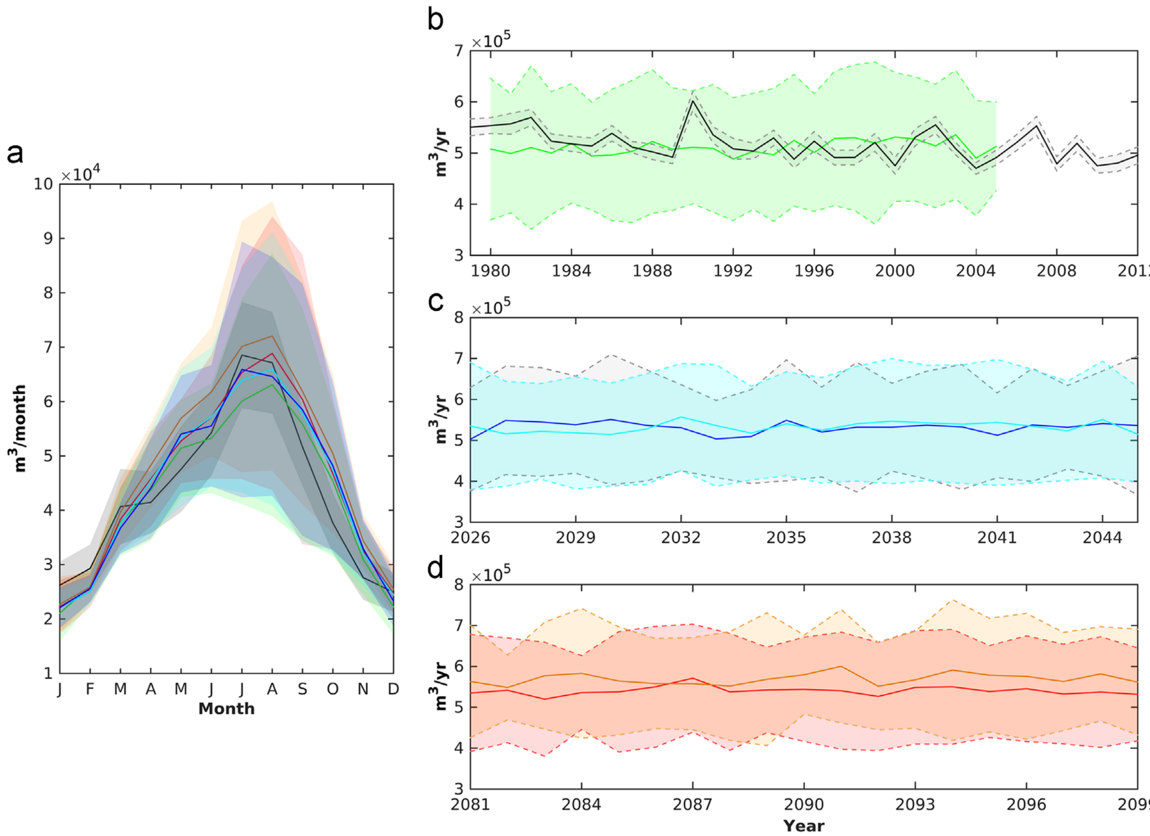

Fig. 10. (a) Seasonal cycle of longshore sediment transport and (b) present, (c) mid, and (d) long-term cumulated annual longshore sediment transport. EraInterim swell wave in black (year-to-year dispersion as shaded zone), model ensemble-average for present, mid and long-term periods in green, blue (RCP4.5 and RCP8.5 in light and dark blue), and red (RCP4.5 in red and RCP8.5 in orange) respectively (model dispersion as shaded zone). Dash lines stand for standard deviation. (For interpretation of the references to color in this figure legend, the reader is referred to the web version of this article.)

COASTVAR (ANR-14-ASTR-0019) and the UNESCO co-chair CIPMA. We benefited from the ECMWF ERA Interim dataset (www.ECMWF.Int/research/Era), SAM index (http://www.nerc-bas.ac.uk/icd/gjma/sam.html), Southern Oscillation Index (http://www.cpc.ncep.noaa.gov/data/indices/soi), Atlantic Nino or Atlantic Meridional Mode (www.esrl.noaa.gov/psd/data/timeseries/monthly/AMM) and future wave scenarios (https://wiki.csiro.au/display/sealevel/COWCLIP), all of which were made freely available. RR is supported by the AXA Research fund and the Deltares Harbour, Coastal and Offshore engineering Research Programme 'Bouwenaan de Kust'.

References

Allan, J.C., Komar, P.D., 2002. Extreme storms on the Pacific Northwest Coast during the 1997–98 El Niño and 1998-99 La Niña. J. Coast. Res. 18, 175–193.
ALOC-GG, 2011. Analyses Littorales, Océaniques et Climatiques au Nord du Golfe de Guinée, organisé par la JEAI ALOC-GG/IRD, Cotonou, Bénin.
Almar, R., Du Penhoat, Y., Hounkonnou, N., Castelle, B., Laibi, R., Anthony, E., Senechal, N., Degbe, G., Chuchla, R., Sohou, Z., Dorel, M., 2014. The Grand Popo experiment, Benin. J. Coast. Res. 70, 651–656 (Special issue).
Anthony, E.J., 1995. Beach-ridge progradation in response to sediment supply: examples from West Africa. Mar. Geol. 129, 175–186.
Anthony, E.J., Blivi, A.B., 1999. Morphosedimentary evolution of a delta-sourced, drift-aligned sand barrier-lagoon complex, western Bight of Benin. Mar. Geol. 158, 161–176.
Anthony, E.J., Oyédé, L.-M., Lang, J., 2002. Sedimentation in a fluvially infilling, barrier-bound, estuary on a wave-dominated, microtidal coast: the Ouémé River estuary, Benin, West Africa. Sedimentology 49, 1095–1112.
Anthony, E.J., 2015. Patterns of sand spit development and their management implications on deltaic, drift-aligned coasts: the cases of the Senegal and Volta River delta spits, West Africa. In: Randazzo, G., Jackson, D.W.T., Cooper, J.A.G. (Eds.), Sand and Gravel Spits, Coastal Research Library Series 12. Springer International Publishing, Switzerland, pp. 21–36. http://dx.doi.org/10.1007/978-3-319-13716-2-2.
Appeaning Addo, K.A., 2009. Detection of coastal erosion hotspots in Accra, Ghana. J. Sustain. Dev. Afr. 4 (11), 253–258.
Appeaning Addo, K.A., Jayson-Quashigah, P.N., Kufogbe, K.S., 2011. Quantitative analysis of shoreline change using medium resolution satellite imagery in Keta, Ghana. Mar. Sci. 1, 1–9.
Arblaster, J.M., Meehl, G.A., Karoly, D.J., 2011. Future climate change in the southern hemisphere: competing effects of ozone and greenhouse gases. Geophys. Res. Lett. 38, L02701. http://dx.doi.org/10.1029/2010GL045384.
Battjes, J.A., Janssen, J.P.F.M., 1978. Energy loss and setup due to breaking of random waves. In: Proceedings of International Conference on Coastal Engineering, ASCE, pp. 569–587.
Bertin, X., Castelle, B., Chaumillon, E., Butel, R., Quique, R., 2008. Alongshore drift estimation and inter-annual variability at a high-energy dissipative beach: St. Trojan Beach, SW Oleron Island, France. Cont. Shelf Res. 28, 1316–1332.
Bidlot, J.-R., Janssen, P.A.E.M., Abdalla, S., 2007. A revised Formulation of Ocean Wave Dissipation and its Model Impact. (ECMWF Technical Report Memorandom 509). ECMWF, Reading (UK).
Blivi, A., 1993. Géomorphologie et Dynamique Actuelle du Littoral du Golfe du Bénin (Afrique de l'Ouest; Thèse). Université Michel de Montaigne, Bordeaux, p. 458.
Bosserelle, C., Pattiaratchi, C., Haigh, I., 2012. Inter-annual variability and longer-term changes in the wave climate of Western Australia between 1970 and 2009. Ocean Dyn. 62 (1), 63–76.
Caires, S., Swail, V.R., Wang, X.L., 2006. Projection and analysis of extreme wave climate. J. Clim. 19 (21), 5581–5605.
CERC, 1984. Shore protection manual, US Army Engineer Waterways Experiment Station, Coastal Engineering Research Center, fourth ed. US Government Printing Office, Washington, D.C..
Chang, E.K.M., Guo, Y., Xia, X., 2012. CMIP5 multimodel ensemble projection of storm track change under global warming. J. Geophys.Res. 117 (D23), D23118.
Charles, E., Idier, D., Thiébot, J., Le Cozannet, G., Pedreros, R., Ardhuin, F., Planton, S., 2012. Present wave climate in the Bay of Biscay: spatiotemporal variability and trends from 1958 to 2001. J. Clim. 25 (6), 2020–2039.
de Coëtlogon, G., Janicot, S., Lazar, A., 2010. Intraseasonal variability of the ocean–atmosphere coupling in the Gulf of Guinea during boreal spring and summer. Q. J. R. Meteorol. Soc. 136 (Suppl. 1), S426–S441 (Special issue).
Davies, J.L., 1980. Geographical Variation in Coastal Development, 2nd Ed. Longman, London, p. 212.
Dee, D.P., et al., 2011. The ERA-interim reanalysis: configuration and performance of the data assimilation system. Q. J. R. Meteorol. Soc. 137, 553–597. http://dx.doi.

org/10.1002/qj.828.
Degbe, C.G., Oyede, L.M., Laibi, R., 2010. Risques environnementaux sur le littoral béninois: érosion côtière et stratégies de lutte. Journées Internationales du Dragage, Libreville. (Unpub).
Delft Hydraulics, 1990. National and regional aspects of coastal erosion in the Bight of Benin. Project 6607.43.94.155, European Development Fund, Brussels.
Fyfe, J.C., 2003. Extratropical southern hemisphere cyclones: harbingers of climate change? J. Clim. 16, 2802–2805.
Gratiot, N., Gardel, A., Anthony, E.J., 2007. Trade-wind waves and mud dynamics on the French Guiana coast, South America: Input from ERA-40 wave data and field investigations. Mar. Geol. 2007 (236), 15–26.
Harley, M.D., Turner, I.L., Short, A.D., Ranasinghe, R., 2011a. A re-evaluation of coastal embayment rotation: the dominance of cross-shore versus alongshore sediment transport processes, Collaroy-Narrabeen Beach, SE Australia. J. Geophys. Res. 116, F0403.
Hemer, M., Chruch, J.-A., Hunter, J.-R., 2010. Variability and trends in the directional wave climate of the Southern Hemisphere. Int. J. Climatol. 30 (4), 475–491.
Hemer, M., Wang, X.L., Weisse, R., Swail, V.R., 2012. Advancing wind-waves climate science: the COWCLIP project. Bull. Am. Meteor. Soc. 93, 791–796.
Hemer, M.A., Yalin, F., Mori, N., Semedo, A., Xiaolan, W.L., 2013. Projected changes in wave climate from a multi-model ensemble. Nat. Clim. Chang. 3, 471–476. http://dx.doi.org/10.1038/nclimate1791.
Hemer, M.A., Trenham, C., 2015. Evaluation of a CMIP5 derived dynamical global wind wave climate ensemble. Ocean Model. (Submitted for publication)
Hoskins, B.J., Hodges, K.I., 2005. A new perspective on Southern hemisphere storm-tracks. J. Clim. 18 (20), 4108–4129.
Inman, D.L., Jenkins, S.A., Elwany, M.H.S., 2001. Wave climate cycles and coastal engineering practice. Coast. Eng. Proc. 25, 314–327. http://dx.doi.org/10.9753/icce.v25, ISSN 2156-1028.
Intergovernmental Panel on Climate Change. (2014). Climate Change 2014: Synthesis Report. Contribution of Working Groups I, II and III to the fifth Assessment Report of the Intergovernmental Panel on Climate Change. [Core Writing Team, R.K. Pachauri adn L.A. Meyer (eds.)]. IPCC, Geneva, Switzerland.
Janicot, S., Caniaux, G., Chauvin, F., de Coëtlogon, G., Fontaine, B., Hall, N., Kiladis, G., Lafore, J.-P., Lavaysse, C., Lavender, S.L., Leroux, S., Marteau, R., Mounier, F., Philippon, N., Roehrig, R., Sultan, B., Taylor, C.M., 2011. Intraseasonal variability of the West African monsoon. Atmosph. Sci. Lett. 12, 58–66.
Kaczmarek, L.M., Ostrowski, R., Pruszak, Z., Rozynski, G., 2005. Selected problems of sediment transport and morphodynamics of a multi-bar nearshore zone. Estuar. Coast. Shelf Sci. 62, 415–425.
Kamphuis, J.W., 1991. Alongshore sediment transport rate. J. Waterw. Port Coast. Ocean Eng. 117 (6), 624–640.
Laibi, R., Anthony, E., Almar, R., Castelle, B., Senechal, N., 2014. Alongshore drift cell development on the human-impacted Bight of Benin sand barrier coast, West Africa. In Proceedings of the 13th International Coastal Symposium. Durban, South Africa. J. Coast. Res. 70, 78–83. (Special issue).
Larson, M., Hoan, L.X., Hanson, H., 2010. A direct formula to compute wave properties at incipient breaking. J. Waterw. Port Coast. Ocean Eng. 136 (2), 119–122.
Longuet-Higgins, M.S., 1970. Alongshore currents generated by obliquely incident sea waves: Jour. Geophys. Res. 75, 6788–6801.
Marshall, G.J., 2003. Trends in the Southern Annular Mode from observations and reanalyses. J. Clim. 16, 4134–4143.
Masselink, G., Short, A.D., 1993. The effect of tide range on beach morphodynamics and morphology: a conceptual model. J. Coast. Res. 9, 785–800.
Masselink, G., Austin, M., Scott, T., Poate, T., Russell, P., 2014. Role of wave forcing, storms and NAO in outer bar dynamics on a high-energy, macro-tidal beach. Mar. Geol. 226, 76–93.
Mendes, D., Souza, E.P., Marengo, J.A., Mendes, M.C.D., 2011. Climatology of extratropical cyclones over the South American-southern oceans sector. Theor. Appl. Climatol. 100 (3–4), 239–250.
Mil-Homens, J., Ranasinghe, R., Van, Thiel, de Vries, J.S.M., Stive, M.J.F., 2013. Re-evaluation and improvement of three commonly used bulk longshore sediment transport formulas. Coast. Eng. 75, 29–39.
MOLOA, 2013. Présentation de la Mission d'Observation du Littoral Ouest Africain (MOLOA), Bulletin de Liaison, Numéro 1, June–July–August, 2013.
Okumura, Y., Xie, S.P., 2004. Interaction of the Atlantic equatorial cold tongue and the African monsoon. J. Clim. 17, 3589–3602.
Ranasinghe, R., McLoughlin, R., Short, A., Symonds, G., 2004. The southern oscillation index, wave climate, and beach rotation. Mar. Geol. 204, 273–287.
Rao, V.B., Do Carmo, A.M.C., Franchito, S.H., 2003. Inter-annual variations of storm tracks in the southern hemisphere and their connections with the Antarctic Oscillation. Int. J. Climatol. 23, 1537–1545.
Richter, I., Xie, S.P., Behera, S.K., Doi, T., Masumoto, Y., 2014. Equatorial Atlantic variability and its relation to mean state biases in CMIP5. Clim. Dyn. 42, 171–188.
Rossi, G., 1989. L'érosion du littoral dans le Golfe du Bénin: un exemple de perturbation d'un équilibre morphodynamique. Z. Geomorphol. 73, 139–165.
Short, A.D., 2012. Coastal processes and beaches. Nat. Educ. Knowl. 3 (10), 15.
Sitarz, J.A., 1960. Côtes africaines: Etude des profils d'équilibre de plage. Travaux du Centre d'Etude et de Recherche en Océanographie. T3, fasc 4, pp. 43–62.
Splinter, K.D., Davidson, M.A., Golshani, A., Tomlinson, R., 2012. Climate controls on alongshore sediment transport. Cont. Shelf Res. 48, 146–156.
Sterl, A., Caires, S., 2005. Climatology, variability and extrema of ocean waves- the web-based KNMI/ERA-40 Wave Atlas. Int. J. Climatol. 25, 963–977.
Stive, M., 2004. How important is global warming for coastal erosion? Clim. Chang. 64, 27–39.
Solari, S., Losada, M.A., 2012. Parametric and non-parametric methods for the study of the variability of wave directions: application to the Atlantic Uruguayan coasts. In: Proceedings of the 33rd International Conference on Coastal Engineering.
Tastet, J.P., Caillon, L., Simon, B., 1985. La dynamique sédimentaire littorale devant Abidjan: impact des aménagements. Contribution à la compréhension des phénomènes d'érosion et de sédimentation UNCI-PAA. p. 39.
Toniazzo, T., Woolnough, S., 2014. Development of warm SST errors in the southern tropical Atlantic in CMIP5 decadal hindcasts. Clim. Dyn. 43 (11), 2889–2913.
Tokinaga, H., Xie, S.-P., 2011. Wave- and anemometer-based sea surface wind (WASWind) for climate change analysis. J. Clim. 24, 267–285.
Tolman, 2009. User manual and system documentation of WAVEWATCH III® version 3.14 NOAA/NWS/NCEP/MMAB Technical Note 276, p. 194.+Appendices.
UEMOA report, 2009. West African Economic and Monetary Union. Regional Programme to Combat Coastal Erosion (PRLEC-UEMOA).
USGS (U.S. Geological Survey) Landsat: A global land-imaging mission (2014) http://landsat.usgs.gov/.
The Wamdi Group, 1988. The WAM model-a third generation ocean wave prediction model. J. Phys. Oceanogr. 18, 1775–1810.
Walcker, R., Anthony, E.J., Cassou, C., Aller, R.C., Gardel, A., Proisy, C., Martinez, J-M, Fromard, F., 2015. Fluctuations in the extent of mangroves driven by multi-decadal changes in North Atlantic waves. Journal of Biogeography . http://dx.doi.org/10.1111/jbi.12580.
Wang, X.L., Swail, V.R., 2006. Climate change signal and uncertainty in projections of ocean wave heights. Clim. Dyn. 26, 109–126.
Wheeler, M., Kiladis, G.N., 1999. Convectively coupled equatorial waves: analysis of clouds and temperature in the wavenumber-frequency domain. J. Atmos. Sci. 56, 374–399.
Woolf, D.K., Challenor, P.G., Cotton, P.D., 2002. Variability and predictability of the North Atlantic wave climate. J. Geophys. Res. 107 (3145).
Wright, L.D., Short, A.D., 1984. Morphodynamic variability of surf zones and beaches: a synthesis. Mar. Geol. 56, 93–118.
Xie, S.P., Carton, J.A., 2004. Tropical Atlantic variability: Patterns, Mechanisms and Impacts. Earth's Clim. Monogr. 147, 121–142.
Yao, K.S., Abe, J., Bamba, S.B., Konan, K.E., Aka, K. 2010. Dynamique d'un périmètre littoral portuaire: la côte de San-Pédro, Sud-Ouest de la Côte d'Ivoire Comptes rendus des Journées Françaises de Génie Cotier-Génie Civil. 3, 2.1–2.12.
Young, I.R., Zieger, S., Babanin, A.V., 2011. Global trends in wind speed and wave height. Science 332, 451.